JOURNAL OF BACTERIOLOGY, May 2010, p. 2512–2524 Vol. 192, No. 10
0021-9193/10/$12.00 doi:10.1128/JB.00058-10

Copper Stress Affects Iron Homeostasis by Destabilizing Iron-Sulfur Cluster Formation in *Bacillus subtilis*▽

Shashi Chillappagari,[1] Andreas Seubert,[1] Hein Trip,[2] Oscar P. Kuipers,[2] Mohamed A. Marahiel,[1] and Marcus Miethke[1]*

Department of Chemistry-Biochemistry, Philipps University Marburg, Hans-Meerwein-Str., D-35032 Marburg, Germany,[1] and Molecular Genetics Group, Groningen Biomolecular Sciences and Biotechnology Institute, University of Groningen, Kerklaan 30, 9751 NN Haren, Netherlands[2]

Received 19 January 2010/Accepted 2 March 2010

Copper and iron are essential elements for cellular growth. Although bacteria have to overcome limitations of these metals by affine and selective uptake, excessive amounts of both metals are toxic for the cells. Here we investigated the influences of copper stress on iron homeostasis in *Bacillus subtilis*, and we present evidence that copper excess leads to imbalances of intracellular iron metabolism by disturbing assembly of iron-sulfur cofactors. Connections between copper and iron homeostasis were initially observed in microarray studies showing upregulation of Fur-dependent genes under conditions of copper excess. This effect was found to be relieved in a *csoR* mutant showing constitutive copper efflux. In contrast, stronger Fur-dependent gene induction was found in a copper efflux-deficient *copA* mutant. A significant induction of the PerR regulon was not observed under copper stress, indicating that oxidative stress did not play a major role under these conditions. Intracellular iron and copper quantification revealed that the total iron content was stable during different states of copper excess or efflux and hence that global iron limitation did not account for copper-dependent Fur derepression. Strikingly, the microarray data for copper stress revealed a broad effect on the expression of genes coding for iron-sulfur cluster biogenesis (*suf* genes) and associated pathways such as cysteine biosynthesis and genes coding for iron-sulfur cluster proteins. Since these effects suggested an interaction of copper and iron-sulfur cluster maturation, a mutant with a conditional mutation of *sufU*, encoding the essential iron-sulfur scaffold protein in *B. subtilis*, was assayed for copper sensitivity, and its growth was found to be highly susceptible to copper stress. Further, different intracellular levels of SufU were found to influence the strength of Fur-dependent gene expression. By investigating the influence of copper on cluster-loaded SufU *in vitro*, Cu(I) was found to destabilize the scaffolded cluster at submicromolar concentrations. Thus, by interfering with iron-sulfur cluster formation, copper stress leads to enhanced expression of cluster scaffold and target proteins as well as iron and sulfur acquisition pathways, suggesting a possible feedback strategy to reestablish cluster biogenesis.

Copper and iron are essential elements employed in pathways that are conserved in all kingdoms of life. In eukaryotes, several interdependent connections between copper and iron homeostasis have been described previously (21). For example, high-affinity iron uptake in *Saccharomyces cerevisiae* is mediated by multicopper-dependent Fet3p and Fet5p converting Fe(II) into Fe(III) (54, 55), and uptake of copper is associated with ferric reductase activity of Fre1p and Fre2p, converting Cu(II) into Cu(I) (16, 22). Further, copper starvation downregulates respiratory functions to preserve iron and copper for other cellular processes (60). In mammals, iron transport from the lumen into the blood circulation is coupled with oxidation of Fe(II) to Fe(III) by the multicopper-ferroxidases hephaestin and ceruloplasmin (45, 62). Fet3p and ceruloplasmin are also involved in copper oxidation to prevent accumulation of the prooxidant Cu(I) (56).

In contrast, investigation of the relationships between iron and copper homeostasis in bacteria has only recently started. While global effects of copper stress on the transcriptome level have been described for model bacteria such as *Escherichia coli* and *Bacillus subtilis* (28, 41), detailed aspects of such connections have been studied so far mainly in *E. coli*. The multicopper oxidase CueO, a laccase-like enzyme present in the periplasm, which was suggested as the site of elevated oxidizable copper levels (35), is responsible for the oxidation of Cu(I) and also the siderophore enterobactin, which is a potential reductant for Cu(II) (17). Catecholate-containing ligands such as enterobactin, the major high-affinity iron scavenger in enteric bacteria (49), are able to reduce Cu(II) into Cu(I), which in turn may further oxidize compounds via formation of reactive oxygen species (ROS) (27). CueO, which is expressed in the presence of copper, oxidizes enterobactin, its catecholate precursors, and its degradation products, leading to the formation of 2-carboxymuconate if 2,3-dihydroxybenzoate is the substrate (18). Another connection between copper and iron homeostasis is the bacterial iron storage protein Dps (58). It protects *E. coli* cells from copper stress, but this is not dependent on presumed functions such as DNA binding or copper storage.

Recently, investigations of the general toxicity effects of copper revealed that Cu(I), the predominant intracellular species (35), destabilizes iron-sulfur cofactors that are weakly bound to

* Corresponding author. Mailing address: Department of Chemistry-Biochemistry, Philipps University Marburg, Hans-Meerwein-Str., D-35032 Marburg, Germany. Phone: 49 6421 2825794. Fax: 49 6421 2822191. E-mail: miethke@staff.uni-marburg.de.

▽ Published ahead of print on 16 March 2010.

TABLE 1. Strains and plasmids used

Strain or plasmid	Genotype or description	Reference or source
B. subtilis strains		
ATCC 21332	Wild type	11
CSP100	Δ*csoR*::*erm*	This study
CSP104	Δ*yhdQ*::*spc*	This study
CSP105	Δ*copA*::*spc*	This study
CSP106	Δ*csoR*::*erm* Δ*yhdQ*::*spc*	This study
AA04	Δ*sufU*::*kan amyE*::pX*sufU*	1
E. coli strains		
TOP10	F$^-$ *mcrA* Δ(*mrr-hsdRMS-mcrBC*) ϕ80*lacZ*ΔM15 Δ*lacX74 deoR nupG recA1 araD139* Δ(*ara-leu*)*7697 galU galK rpsL* (Str^r) *endA1* λ$^-$	Invitrogen
BL21(DE3)	F$^-$ *ompT gal dcm lon hsdS*$_B$(r_B^- m_B^-) λ(DE3)	Novagen
Plasmids		
pUS19	Donor of antibiotic resistance cassette; Spc^r	7
pMUTIN	Donor of antibiotic resistance cassette; Erm^r	59
pET28a_sufU	pET28a(+) containing an N-terminal His$_6$ tag fusion of *sufU*	1

dehydratases of primary metabolism (34). Dihydroxy-acid dehydratase (IlvD) in the common branched-chain amino acid synthesis pathway and isopropylmalate dehydratase (LeuC) in the leucine-specific branch, as well as fumarase A (FumA) and 6-phosphogluconate dehydratase (Edd), were found to be affected *in vivo*, and fumarase A was also found to be affected during studies *in vitro*. In this context, it was also shown that an *E. coli sufABCDSE* mutant was more susceptible to copper stress, indicating that the *E. coli* SUF system for iron-sulfur cluster assembly contributes to copper resistance.

Much less is known about associations of copper and iron pathways in Gram-positive bacteria. In the soil-dwelling model bacterium *B. subtilis*, these pathways have been separately investigated in recent studies. *B. subtilis* employs bacillibactin as an endogenous high-affinity iron scavenger and has further uptake capacities for hydroxamate siderophores and elemental iron (38, 44). The bacillibactin pathway comprises the *dhbACEBF* genes for bacillibactin synthesis (37), *ymfE* (renamed *ymfD* upon genome resequencing), encoding a major facilitator superfamily transporter for bacillibactin export (6, 39), *feuABC-yusV*, coding for an ABC-type transporter that mediates Fe-bacillibactin uptake, and *besA*, which permits intracellular hydrolysis of the siderophore trilactone backbone (38, 44, 47). Except for the bacillibactin exporter gene, these genes are part of the Fur regulon, which responds to intracellular iron limitation (3). Other systems of iron homeostasis include iron storage proteins, also called "miniferritins," which are encoded by *dps* and *mrgA* (8, 9), as well as the recently described SUF-type system for iron-sulfur cluster maturation (1). The *B. subtilis* SUF system is encoded by the *sufCDSUB* gene cluster, and *sufU* was found to be the major scaffold protein used for cluster assembly and transfer to target proteins.

On the other hand, *B. subtilis* copper homeostasis is controlled mainly by the global regulator CsoR, which targets both copper efflux and influx (10, 53). The copper efflux operon *copZA* codes for the CopZ copper chaperone and the CopA efflux pump, which act together (5), while the gene *ycnJ* codes for a copper uptake system, which is further negatively regulated by YcnK (10). Another copper chaperone, YpmQ, was found to be essential for cytochrome maturation (36). YhdQ (CueR), a MerR-type regulator, was found to bind to the *copZA* promoter as well, but the physiological relevance of this is uncertain (53).

The current study describes the effects of environmental copper excess primarily on iron homeostasis in *B. subtilis*. Microarray studies revealed different regulatory patterns of iron homeostasis genes depending on the intracellular copper content in different strains affected in copper homeostasis. Not only iron acquisition genes but also genes encoding iron-sulfur cluster scaffolding proteins and target enzymes of iron-sulfur cofactors were found to be affected. Direct effects observed for copper and iron-sulfur cluster assembly on SufU and altered expression of iron acquisition genes depending on intracellular amounts of SufU provide evidence that iron-sulfur biogenesis is a primary target of copper toxicity and indicate that the global changes of iron homeostasis are driven by an enhanced requirement for iron for iron-sulfur cluster formation under copper stress.

MATERIALS AND METHODS

Bacterial strains, plasmids, and growth media. The bacterial strains and plasmids used in this study are listed in Table 1. *B. subtilis* strains were grown in Belitsky minimal medium (BMM) under constant shaking at 250 rpm and 37°C. BMM was supplemented with 0.5% (wt/vol) glucose as a carbon source, 0.45 mM glutamate, and all vital nutrients required, including 1 μM $FeSO_4$ (57). In studies including the *sufU* conditional mutant, glucose was replaced by 0.2% fructose as a C source for all strains, and various concentrations of xylose were added to trigger P_{xyl}-dependent *sufU* expression (1). Copper excess conditions were maintained by adding freshly prepared CuCl or $CuSO_4$ at a 0.5 mM final concentration if not indicated otherwise. Fresh liquid medium for growth under different copper conditions was inoculated from an overnight preculture that was grown at 37°C with constant shaking at 225 rpm. Special care was taken to wash the glassware additionally with 0.1 M HCl and double-distilled water before autoclaving. The antibiotics erythromycin (1 μg ml^{-1}), lincomycin (25 μg ml^{-1}), and spectinomycin (100 μg ml^{-1}) were used for the selection of *B. subtilis* mutant strains. *E. coli* strains were grown in LB medium. For selection of *E. coli* Top10 strains containing transformed plasmids, the antibiotic kanamycin (50 μg ml^{-1}) was used. *E. coli* BL21 was used for protein overexpression. For RNA preparations, bacteria were harvested at the mid-log growth phase.

DNA manipulations and genetic techniques. DNA preparations and transformations were carried out as described previously (24, 52). Electroporation was used for the transformation of plasmids into *E. coli* cells. Natural competence obtained by high-salt/low-salt treatment was used for transformations of *B. subtilis* ATCC 21332 during mutant constructions (29). Restriction enzymes, T4

TABLE 2. Primers used to create mutants and riboprobes

Function and primer name	Primer sequence (5′ to 3′)[a]
Mutant construction	
Csp100-Δ*csoR*-Us-FP	CCACATGACGAAGCAACTTCGTACAG
Csp100-Δ*csoR*-Us-RP	GCAAGTCAGCACGAACACGAACCGCTTTTATGGTTTAATGTTTTATGTTCGTTATGCTTTTCCAT
Csp100-Δ*csoR*-Ds-FP	GTCTATTTTTAATAGTTATCTATTATTTAACGGGAGGAAATAAGGGGAACAGGCCATTTCTGAGC
Csp100-Δ*csoR*-Ds-RP	GGCTTCCCGTTTGTCACGGTTCC
Csp104-Δ*yhdQ*-Us-FP	CTAAGCAGAGGGCCCCATCATACC
Csp104-Δ*yhdQ*-Us-RP	CTCTTGCCAGTCACGTTACGTTATTAGTTGAGTGCCGCTAGTTCACTGATGCG
Csp104-Δ*yhdQ*-Ds-FP	CTATAAACTATTTAAATAACAGATTAAAAAAATTATAAAGCAAACTCCCGCCTGAAAAGCTC
Csp104-Δ*yhdQ*-Ds-RP	GCAGCCCTCTTCGATGATGGAATC
Csp105-Δ*copA*-Us-FP	GCTCATGTACAACCTCAGCATCTGG
Csp105-Δ*copA*-Us-RP	CTCTTGCCAGTCACGTTACGTTATTAGCAACATACTCACTCCTTTATATACACCTGG
Csp105-Δ*copA*-Ds-FP	CTATAAACTATTTAAATAACAGATTAAAAAAATTATAAGGCTATATGCCGGTTTTTGTTTTTCATTGACAC
Csp105-Δ*copA*-Ds-RP	GCAGAACGCCGTTTTGATTGATAAAGCC
Riboprobe construction	
FP RP *dhbB*	GCGCGTTTAAGAGAACGAATCTGC
RP RP *dhbB*	**TAATACGACTCACTATAGG**GTTTGCTGACGTTTTTTGAACGTCTGC
FP RP *dhbF*	GCATTCACCATATAGCGATCGACG
RP RP *dhbF*	**TAATACGACTCACTATAGG**GCGCCGCTTCTTTTAACGCGTTTAC
FP RP *feuB*	CGGTGTTAGTATTCGGCCTTGC
RP RP *feuB*	**TAATACGACTCACTATAGG**GGCACTGCCGGTTAGAATGATG
FP RP *feuC*	GCTCTTATTCCAAGGCCAGAAGG
RP RP *feuC*	**TAATACGACTCACTATAGG**GCTTCCGTTTTTCCACACCATGG
FP RP *besA*	CCTGTGATTTATCTGCTGGATGCC
RP RP *besA*	**TAATACGACTCACTATAGG**GAGCGAATGGCCAAAGATTGTTTG

[a] Underlining indicates the complementary resistance cassette overlaps for mutant construction. Bold indicates T7 promoter regions in riboprobe primers.

DNA ligase, and calf intestinal phosphatase were used according to the manufacturer's instructions (New England Biolabs).

Mutant construction. *B. subtilis* deletion mutants were generated by introducing PCR fusions of resistance marker cassettes and chromosomal long flanking homology regions (63). Long flanking homologous fragments were amplified from upstream and downstream regions of the target genes using primers listed in Table 2. The 3′ ends of the resulting upstream and downstream PCR products were designed to be complementary to the 3′ ends of the fused resistance cassette. Hybrid constructs were obtained by using the flankers as primers during the fusion PCR. After purification, constructs were transformed into the wild-type (WT) strain, and gene deletion mutants were selected on antibiotic plates. All PCRs were performed with Platinum *Pfx* DNA polymerase (Invitrogen). Deletions of the genes were confirmed by PCR using isolated chromosomal DNAs of selected transformants as templates. The erythromycin resistance cassettes used for the construction of the Δ*csoR* mutant was amplified from the pMUTIN vector. To generate the Δ*yhdQ* and Δ*copA* mutants, the spectinomycin resistance cassette from the pUS19 vector was used.

Microarray experiments. To perform microarray experiments, ATCC 21332 WT, Δ*csoR*, and Δ*csoR* Δ*yhdQ* mutant strains were grown in BMM under normal conditions (no copper added) and under copper-replete conditions (with addition of freshly prepared 0.5 mM CuCl). Cultures were harvested in the mid-log phase for RNA extraction. The Macaloid/Roche method was used for the RNA extraction (30). Concentrations of RNA were measured using the nanodrop method. For reverse transcription, a solution containing 18 μl annealing mix (10 to 20 μg total RNA, 2 μl random nonamers adjusted to the final volume of 18 μl with nuclease-free water) was incubated for 5 min at 70°C and for 10 min at 4°C for annealing. Reverse transcription was performed by addition of this annealing mix to a solution containing 6 μl Superscript III buffer (supplied with the reverse transcriptase), 10 mM dithiothreitol (DTT), nucleotide master mix containing aminoallyl-dUTP, and 300 U Superscript III reverse transcriptase (Invitrogen). cDNA was synthesized overnight at 42°C in a total volume of 30 μl. The aminoallyl-modified cDNA was incubated with the CyDye *N*-hydroxysuccinimide (NHS) ester (Cy3 or Cy5 monoreactive dye) at room temperature in the dark for 60 to 90 min. Labeled cDNAs were purified using Nucleo Spin Extract II columns, and the dye incorporation was measured using the nanodrop method. Equal quantities of Cy3/Cy5-incorporated cDNAs were mixed, dried via vacuum centrifugation, and then dissolved in 5 μl H_2O, followed by heating at 94°C for 2 min. The heated sample was subsequently mixed with 30 μl preheated hybridizing buffer (68°C), hybridized onto microarray glass slides, and incubated overnight at 68°C in a hybridization oven.

Microarray data analysis. Hybridized DNA arrays were read using a GenePix autoloader 4200AL (Axon Instruments), and the data obtained were processed with ArrayPro 4.5 (Media Cybernetics Inc., Silver Spring, MD) ArrayVision software. Expression levels were processed and normalized (Lowess method) with Micro-Prep software (15, 61). The ln-transformed ratios of the expression levels were subject to a *t* test using the Cyber-T analysis tool (4). Three independent measurements for each condition along with an additional dye swap were analyzed. The results obtained were averaged, and significant expression ratios of >1.5 for all upregulated genes and <0.7 for all downregulated genes were set with a general pBayes reliability of $<10^{-3}$.

Dot blot analysis. *B. subtilis* strains were grown in BMM without (control) or with addition of copper (0.5 mM). In studies with the *sufU* conditional mutant, 0.2% fructose was used as a C source, and various concentrations of xylose as inducer were added. Inoculation of fresh medium to an initial optical density at 600 nm (OD_{600}) of 0.05 was done with overnight precultures. Cells were harvested at an OD_{600} of 0.25, and total RNA was isolated from these cells using the RNAZol method. RNA-to-protein ratios were determined using the nanodrop method at 260 nm/280 nm. The RNA-to-protein ratios were above 1.65 in all samples. Denaturing gel electrophoresis was done to test the RNA quality for 16S and 23S rRNAs. Two micrograms of RNA from each sample was subsequently dotted onto the nylon membrane using a dot blot apparatus and hybridized after UV cross-linking with a UTP-11-digoxigenin-labeled antisense RNA probe. Riboprobes specific for *dhbB*, *dhbF*, *feuB*, *feuC*, and *besA* transcripts were synthesized by *in vitro* transcription using T7 RNA polymerase and primers listed in Table 2. After hybridization and washing, the filters were treated with a digoxigenin-specific antibody fragment conjugated with alkaline phosphatase (Roche) and AttoPhos (Amersham Biosciences) as an enhanced chemifluorescence (ECF) substrate. The hybridization signals were detected with a Storm860 fluorescence imager, and relative signal quantification was performed with ImageQuant software.

Western blot analysis. *B. subtilis* WT cells were grown in BMM with 0.2% fructose and different concentrations of copper. The *sufU* conditional mutant was grown in minimal medium with 0.2% fructose and different concentrations of xylose as an inducer of the P_{xyl} promoter. Cultures were harvested at an OD_{600} of 0.8, cells were disrupted by sonication, and cytosolic protein extracts (25 μg total protein per lane) were separated by SDS-PAGE prior to blotting onto nylon membranes. SufU was detected by using specific polyclonal antibodies from rabbit and goat anti-rabbit IgG conjugated with alkaline phosphatase as a secondary antibody.

TABLE 3. Effects of copper stress on CsoR and Fur regulation in WT, Δ*csoR*, and Δ*csoR* Δ*yhdQ* strains

Category and gene	Induction ratio[a]			Gene function[b]
	WT (Cu/co)	Δ*csoR*/WT (Cu)	Δ*csoR* Δ*yhdQ*/WT (Cu)	
CsoR-regulated genes				
copA	**2.6**	**6.4**	**6.3**	Copper efflux pump
copZ	NS	**4.2**	**5.2**	Copper efflux chaperone
ycnJ	0.4	**2.3**	**3.2**	Copper uptake pump
ycnK	0.3	**1.9**	**4.9**	Copper uptake regulator
Fur-regulated genes				
dhbA	**1.5**	0.4	0.4	2,3-Dihydro-2,3-dihydroxybenzoate dehydrogenase
dhbB	**2.7**	0.3	0.2	Isochorismatase
dhbC	**1.7**	0.4	0.2	Isochorismate synthase
dhbE	**2.2**	0.3	0.2	2,3-Dihydroxybenzoate adenylation
dhbF	**2.3**	0.3	0.1	Bacillibactin biosynthesis
feuA	**2.8**	0.6	0.3	Ferribacillibactin binding protein
feuB	**2.3**	0.7	0.6	Ferribacillibactin uptake (integral membrane protein)
feuC	1.2	0.7	0.7	Ferribacillibactin uptake (integral membrane protein)
yusV	1.3	0.7	0.7	Ferribacillibactin uptake (ATPase unit)
besA	**2.1**	0.3	0.3	Ferribacillibactin trilactone hydrolase
btr	**1.6**	0.8	0.9	Regulator of ferribacillibactin uptake

[a] Shown are mean induction ratios from four independent transcriptome comparisons. Cu, copper excess; co, control without added copper. Bold indicates ratios showing at least 1.5-fold upregulation, and underlining indicates ratios showing at least 1.5-fold downregulation. NS, no significant ratio based on pBayes statistical analysis.

[b] Gene functions are taken from the SubtiWiki database (13).

Determination of intracellular copper and iron concentrations. WT *B. subtilis* strain ATCC 21332 and the Δ*csoR* and Δ*copA* mutants were grown in BMM overnight. Fresh BMM (100 ml) either with 0.5 mM copper (excess) or without copper (control) was inoculated with overnight cultures with a starting OD_{600} of 0.05, and the cells were harvested in mid-log phase. Cells were centrifuged at 18,000 × *g* for 5 min, and the pellets were washed three times with buffer containing 10 mM Tris-HCl and 1 mM EDTA (pH 7.5) and finally with MilliQ-water to remove extracellular traces of salt. Cells were dried overnight at 85°C and treated with suprapure nitric acid for quantitative breaking, and intracellular metal contents were analyzed by inductively coupled plasma mass spectrometry (ICP-MS) using an Agilent 7500ce ICP-MS.

Quantification of intracellular NAD and NADH. Estimation of nicotinamide levels in the cells was done following published protocols (33). Briefly, the Δ*csoR* deletion mutant strain was grown in parallel with the WT in BMM under the desired conditions. Cells were harvested at an OD_{600} of 0.6 at 4°C, and pellets were either shock frozen in liquid nitrogen for later use or directly processed. Cells were washed once with ice-cold 50 mM phosphate buffer (KH_2PO_4, pH 7.0; adjusted with KOH) and then resuspended in 5 to 7 ml of 0.1 M Tris-HCl, pH 8.2. To differentiate between oxidized and reduced nicotinamide levels, the suspension was divided into two equal portions of 3 ml each. The first portion was used to extract the oxidized forms (NAD^+) by adding 1.5 ml of 0.33 N HCl, and the second portion was used to extract reduced forms (NADH) by adding 1.5 ml of 0.33 N NaOH. Both samples were incubated in a water bath maintained at 50°C for 10 min. Extracts were cooled to 0°C, and samples were neutralized by adding 0.45 ml of 1 N NaOH to portion 1 and 0.45 ml of 1 N HCl to portion 2. Care was taken to avoid local concentrations of acid or alkali by dropwise addition with continuous shaking. Insoluble material was removed at 23,000 × *g* for 15 min. Further, reoxidation of NAD^+ in the second portion was performed by adding 10 μl of 146-mg/ml 2-oxoglutarate–53.3 mg of NH_4Cl (pH 7) adjusted with NaOH and 10 μl of glutamic dehydrogenase (Sigma; ~40 units/mg) and incubating at room temperature for 15 min. Reoxidized nicotinamides were extracted by the addition of 100 μl of 5 N HCl and incubation for 15 min at 50°C followed by neutralization with 90 μl of 5 N NaOH. Precipitates were removed at 23,000 × *g* for 15 min. To analyze the nicotinamide levels, 2 ml of 0.1 M pyrophosphate-semicarbazide buffer (containing 100 ml of 0.11 M sodium pyrophosphate, 5 ml of l M semicarbazide hydrochloride, and 5 ml of 1 M glycine, pH 8.8; adjusted with NaOH) was added to 1 ml of clarified extracts, and 10 μl ethanol was added as a substrate. After the blank was measured at 340 nm, 10 μl of alcohol dehydrogenase (Sigma; ~300 units/mg) was added. Reaction mixtures were incubated at room temperature for 10 min to allow total conversion, and final values were measured at 340 nm.

***In vitro* experiments with recombinant SufU.** Recombinant SufU was overproduced and purified as described previously (1). Briefly, cultures were induced at an OD_{600} of 0.5 to 0.7 with 0.5 mM IPTG (isopropyl-β-D-thiogalactopyranoside) for 4 h at 37°C. After being harvested, the cells were resuspended in 50 mM HEPES–300 mM NaCl (pH 8.0) and disrupted by using a French press (Sim Aminco) at 10,000 lb/in^2. After removal of the cell debris (by centrifugation at 34,000 × *g* at 4°C), the supernatant was loaded on an Ni^{2+}-nitrilotriacetic acid (NTA) column (Qiagen). Elution was performed with a linear gradient (0 to 100%) of 50 mM HEPES, 300 mM NaCl, and 250 mM imidazole (pH 8.0) at a flow rate of 1 ml per min over 50 min using a fast protein liquid chromatography (FPLC) system (Amersham Pharmacia Biotech). The sample fractions were analyzed by SDS-PAGE, and fractions with the highest protein yields were pooled, concentrated, and dialyzed using Amicon Ultra-15 centrifugal filter units (Millipore) with a 10,000-molecular-weight cutoff. For cluster reconstitution, SufU (50 μM, 1 mg/ml) was reduced anaerobically (95% N_2–5% H_2 atmosphere) with 5 mM DTT in 25 mM Tris-HCl–100 mM NaCl (pH 8.0) for 1 h. Ferric ammonium citrate was then added at a stoichiometry of 4:1 (iron to protein) and incubated for approximately 10 min until the observed color change to red was stable. An equal amount of Li_2S was added slowly, and the sample was incubated for 15 min before unbound iron and sulfide were removed via size exclusion chromatography over a PD-10 column equilibrated in 25 mM Tris-HCl–100 mM NaCl (pH 8.0) containing 0.5 mM DTT. Reconstituted holo-SufU was then titrated anaerobically with Cu(I) or Cu(II), and UV/visible absorption spectra were recorded on a Jasco V-550 spectrophotometer.

RESULTS

Deregulation of iron uptake and amino acid metabolism under copper stress. Microarray studies performed with the WT strain and copper efflux mutants under conditions of copper excess (0.5 mM copper supplementation) showed effects on both copper and iron homeostasis gene expression. Genes of the *cop* operon for copper efflux were upregulated about 2- to 3-fold, and genes *ycnJK*, involved in copper influx, were downregulated with similar ratios in the WT under copper excess, as expected under conditions requiring copper detoxification (Table 3). Further, Fur-regulated genes for high-affinity iron uptake, especially via the bacillibactin pathway, were

generally upregulated (Table 3). However, when a copper-stressed *csoR* knockout mutant was compared with the WT under the same conditions, this regulatory pattern was found to be inverted. Thus, derepression of Fur-regulated genes appeared to be significantly less strong in the copper-stressed Δ*csoR* strain. Since expression of iron acquisition genes was not found to be altered when the transcriptome profiles of the Δ*csoR* and WT strains were compared under normal conditions (data not shown), it was excluded that CsoR may have a direct regulatory effect on expression of these targets. Thus, we speculated that this effect was based on higher copper efflux capacities in the Δ*csoR* strain. Indeed, the mutant showed 4- to 6-fold-higher induction of copper detoxification genes *copZA* than the WT under copper stress conditions (Table 3). Further, when the transcriptomes of copper-stressed WT and Δ*csoR* Δ*yhdQ* double mutant strains were compared, even stronger derepression rates of iron uptake genes were observed in the knockout strain, suggesting possible additive effects of CsoR and YhdQ in regulation of copper detoxification. Although the function of YhdQ was revised to be directly involved in transcriptional regulation of the *B. subtilis cop* operon (53), this proposed regulator was found to bind to its promoter region and hence could still contribute at least indirectly to local regulation. Thus, the array data indicated that copper stress induces genes required for iron uptake, while enhanced copper detoxification is a determinant that prevents upregulation of these genes.

Further, expression of two exemplary Fur-regulated genes, *dhbB* and *feuB*, was analyzed by dot blot hybridization using WT and Δ*csoR* and Δ*copA* mutant strains under control and copper stress conditions (Fig. 1). According to the microarray data, the WT and Δ*csoR* strains did not show significant alterations in Fur-dependent gene expression under control conditions; however, expression of these genes was found to be higher in the WT under copper stress. The Δ*copA* mutant, on the other hand, having blocked copper efflux, showed upregulation under both control and, with a further increase, copper stress conditions. These data indicated that deregulation of Fur-dependent expression corresponds to the cellular capacity of copper efflux, in particular under conditions of elevated copper stress.

A further observation was made regarding the expression pattern of amino acid pathways. Pathways upregulated under copper stress included those of cysteine and branched-chain amino acid biosynthesis (Table 4). These pathways were found to be considerably less induced or even partially downregulated in the Δ*csoR* mutant under copper stress. Almost complete downregulation of all pathway genes was observed when the Δ*csoR* Δ*yhdQ* mutant was compared with the WT under copper stress. Thus, in addition to iron acquisition, the capability for copper efflux also had a strong impact on specific amino acid pathways. Interestingly, arginine biosynthesis was found to be most strongly downregulated in the WT during copper stress, while it was greatly upregulated in the Δ*csoR* Δ*yhdQ* mutant compared with the WT under copper excess. The deregulation of amino acid pathways will be discussed with the data presented below.

Copper stress does not release a global oxidative stress response. To investigate the association between copper stress and Fur derepression, it was first assumed that an oxidative stress response might be induced, which may occur due to formation of ROS in a Fenton-like reaction involving Cu(I). As previously reported, both peroxide and superoxide stresses lead to the induction of the PerR and Fur regulons, and the PerR regulon comprises genes for detoxification of ROS and DNA protection in *B. subtilis* (43). In this context, the highest induction ratios in the presence of both peroxide and superoxide stresses have been found for the vegetative catalase gene *katA* and the DNA protection protein gene *mrgA*. In the present study, however, the majority of these genes were found not to be induced under copper stress conditions in the WT relative to the control or enhanced copper efflux in the copper-stressed Δ*csoR* mutant (Table 5). Indeed, only four PerR-regulated genes were found to be induced under copper stress, including *ahpC* and *ahpF*, coding for reduction of alkyl hydroperoxides, and *yuiA* and *yuiB*, with unknown functions. All other genes of the oxidative stress regulon were not significantly affected. Further, oxidative stress genes coding for proteins that contain iron as a cofactor, such as *katA* or *sodF*, were not upregulated during copper stress and hence are not likely to represent targets for copper-induced iron acquisition. In

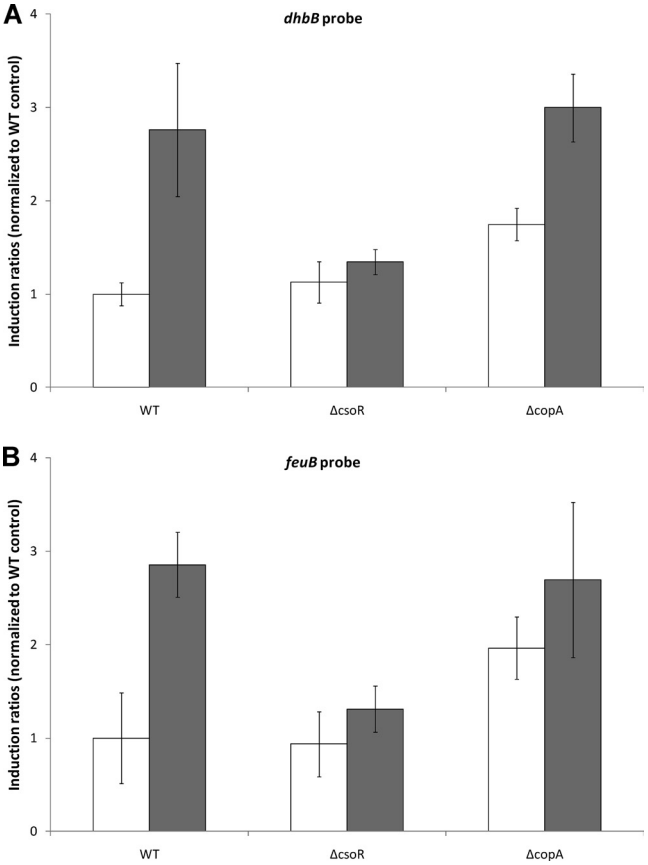

FIG. 1. Relative expression levels of *dhbB* (A) and *feuB* (B) with different copper levels. Total RNA was isolated from mid-log-phase *B. subtilis* WT, Δ*csoR*, and Δ*copA* cells grown in minimal medium without addition of copper (white bars) or with 0.5 mM copper (gray bars) and analyzed by dot blot hybridization using specific mRNA antisense probes. The signals obtained were quantified with ImageQuant software, and the induction ratios were normalized to the WT control (set to 1.0). Error bars indicate standard deviations.

TABLE 4. Effects of copper stress on amino acid biosynthesis genes in WT, Δ*csoR*, and Δ*csoR* Δ*yhdQ* strains

Category and gene	Induction ratio[a]			Gene function[b]
	WT (Cu/co)	Δ*csoR* (Cu/co)	Δ*csoR* Δ*yhdQ*/WT (Cu)	
Cysteine biosynthesis				
cysC	**7.7**	0.9	0.3	Probable adenylylsulfate kinase
cysH	**4.2**	**1.6**	0.2	3′-Phosphoadenylylsulfate reductase
cysK	**3.0**	0.2	0.2	Cysteine synthetase A
cysP	**2.7**	0.1	0.3	Sulfate permease
cysE	**1.5**	1.2	0.6	Serine acetyltransferase
sat	**6.3**	0.5	0.2	Probable sulfate adenylyltransferase
ylnD	**6.5**	0.7	0.2	Similar to uroporphyrin-III C-methyltransferase
ylnE	**3.5**	1.2	0.4	Unknown, part of *cysH* operon
mccA (*yrhA*)	**3.3**	0.6	1.1	*O*-Acetylserine-thiol-lyase (cysteine synthase)
mccB (*yrhB*)	1.2	1.4	0.5	Cystathionine gamma-lyase
cysI (*yvgR*)	**1.6**	1.4	0.7	Sulfite reductase
cysJ (*yvgQ*)	**1.7**	0.4	0.7	Sulfite reductase
Leucine biosynthesis				
leuA	**1.5**	0.8	0.7	2-Isopropylmalate synthase
leuB	**2.2**	**1.5**	0.5	3-Isopropylmalate dehydrogenase
leuC	**2.2**	1.0	0.8	3-Isopropylmalate dehydratase (large subunit)
leuD	**2.2**	1.2	0.5	3-Isopropylmalate dehydratase (small subunit)
Isoleucine/valine biosynthesis				
ilvA	**1.8**	**1.5**	0.5	Threonine dehydratase
ilvB	**2.4**	0.3	0.6	Acetolactate synthase (large subunit)
ilvC	**1.5**	0.9	0.7	Ketol-acid reductoisomerase
ilvD	**2.6**	0.9	0.6	Dihydroxy-acid dehydratase
ilvH	**2.2**	0.7	0.5	Acetolactate synthase (small subunit)
Arginine biosynthesis				
argG	0.2	0.7	**15.0**	Argininosuccinate synthase
argJ	0.2	1.4	**10.5**	Ornithine acetyltransferase/amino acid acetyltransferase
argD	0.2	0.6	**9.2**	*N*-Acetylornithine aminotransferase
argB	0.2	0.4	**7.1**	*N*-Acetylglutamate 5-phosphotransferase
argC	0.2	**2.5**	**6.2**	*N*-Acetylglutamate gamma-semialdehyde dehydrogenase
argH	0.1	0.9	**13.6**	Argininosuccinate lyase
argF	0.1	0.3	**23.5**	Ornithine carbamoyltransferase
carA	0.2	0.9	**13.2**	Carbamoyl-phosphate transferase-arginine (subunit A)
carB	0.2	0.6	**14.5**	Carbamoyl-phosphate transferase-arginine (subunit B)
artP (*yqiX*)	0.1	0.1	**16.8**	Arginine transport (binding protein)
artQ (*yqiY*)	0.4	0.7	**6.3**	Arginine transport (permease)
artR (*yqiZ*)	0.4	**1.6**	**5.7**	Arginine transport (ATP binding protein)

[a] Shown are mean induction ratios from four independent transcriptome comparisons. Cu, copper excess; co, control without added copper. Bold indicates ratios showing at least 1.5-fold upregulation, and underlining indicates ratios showing at least 1.5-fold downregulation.
[b] Gene functions are taken from the SubtiWiki database (13).

contrast, genes under the control of the Rex (YdiH) regulator, which senses the ratio of intracellular NADH to NAD (31, 50), were significantly affected (Table 5). Under relative copper limitation in the Δ*csoR* mutant compared to the WT under copper excess, genes of the cytochrome family and genes involved in cytochrome synthesis as well as genes encoding NADH-dependent lactate dehydrogenase and lactate permease were induced. Since NADH levels are expected to be linked with the copper-dependent cytochrome system, the NADH/NAD ratios in the copper-stressed WT and Δ*csoR* mutant strains were determined and found to be 0.9 and 3.4, respectively. Thus, copper-dependent recycling of NADH was significantly affected in the Δ*csoR* mutant under copper stress compared to the corresponding WT conditions. In the copper-stressed WT compared with the control, Rex-dependent genes were downregulated, including *cydA* and *cydB*, coding for iron-dependent cytochrome biosynthesis. Together, these data suggest that copper excess leads to significant changes in cellular energy metabolism, which, however, are not associated with elevated levels of oxidative stress, including iron-dependent ROS detoxification or increased levels of iron-dependent cytochrome utilization.

Copper-induced Fur derepression is related to high intracellular copper content. To determine the overall intracellular levels of copper present in the WT and the Δ*csoR* and Δ*copA* mutants, ICP-MS measurements of total cell fractions were carried out with cells cultured under different growth conditions. Differences in intracellular copper levels were detected in the WT, Δ*csoR*, and Δ*copA* strains under normal and copper excess conditions (Table 6). While in the WT and Δ*csoR* mutant strains, copper contents were similarly low under normal conditions, Δ*copA* cells had an about a 1,000-fold-higher copper content. Under conditions of copper excess, the copper content drastically increased in all strains, but with an 800-fold

TABLE 5. Effects of copper stress on PerR and Rex (YdiH) regulation in WT and Δ*csoR* strains

Category and gene	Induction ratio[a]		Gene product with iron cofactor	Gene function[b]
	WT (Cu/co)	Δ*csoR*/WT (Cu)		
PerR-regulated genes				
katA	0.8	1.2	Yes	Vegetative catalase 1
mrgA	0.7	**1.5**	Yes	Metalloregulation DNA-binding stress protein
ahpC	**2.2**	0.9	No	Alkyl hydroperoxide reductase (small subunit)
ahpF	**2.3**	0.9	No	Alkyl hydroperoxide reductase (large subunit)
hemA	0.8	1.2	No	Glutamyl-tRNA reductase
hemX	1.4	0.9	No	Negative effector of the concn of HemA
hemC	1.0	1.0	No	Porphobilinogen deaminase
hemD	1.1	1.0	No	Uroporphyrinogen III cosynthase
hemB	0.9	1.2	No (zinc)	Delta-aminolevulinic acid dehydratase
hemL	0.9	0.9	Yes	Glutamate-1-semialdehyde 2,1-aminotransferase
fur	1.0	1.1	Yes	Transcriptional repressor of iron uptake
perR	1.1	1.3	Yes	Transcriptional repressor of the peroxide regulon
iseA (*yoeB*)	0.2	**2.0**	Not predicted	Protection against cell envelope stress
yuiA	**2.1**	0.9	Not predicted	Unknown
yuiB	**3.2**	0.8	Not predicted	Unknown
zosA (*ykvW*)	1.0	1.1	No (zinc)	Similar to heavy metal-transporting ATPase
Other oxidative stress genes				
sodA	**1.5**	1.3	No (manganese)	Superoxide dismutase
sodF	0.8	1.0	Yes	Superoxide dismutase
yojM	1.2	0.9	No (zinc)	Similar to superoxide dismutase
Rex-regulated genes				
ldh	0.3	**7.2**	No	L-Lactate dehydrogenase
lctP	0.3	**5.9**	No	L-Lactate permease
ywcJ	0.3	**3.8**	No	Similar to nitrite transporter
cydA	0.7	**2.0**	Yes	Cytochrome *bd* ubiquinol oxidase (subunit I)
cydB	0.3	**4.9**	Yes	Cytochrome *bd* ubiquinol oxidase (subunit II)
cydC	0.6	**2.4**	No	ABC transporter required for expression of cytochrome *bd* (ATP binding protein)
cydD	0.9	NS	No	ABC transporter required for expression of cytochrome *bd* (ATP binding protein)

[a] Shown are mean induction ratios from four independent transcriptome comparisons. Cu, copper excess; co, control without added copper. Bold indicates ratios showing at least 1.5-fold upregulation, and underlining indicates ratios showing at least 1.5-fold downregulation. NS, no significant ratio based on pBayes statistical analysis.

[b] Gene functions are taken from the SubtiWiki database (13).

difference between the WT and Δ*csoR* strains. The differences in intracellular copper content were found to correspond to the observed pattern of induction of Fur-regulated genes. In contrast, the intracellular iron content was found to be in the same range in WT and mutant cells under normal and copper excess conditions. Thus, Fur derepression under copper stress did not depend on changes in the total intracellular iron content. Due to the broad differences in intracellular copper levels under normal conditions and copper stress, it seemed unlikely that derepression was caused by direct effects on transcriptional regulation such as inactivation of the Fur repressor, as previously suggested (41). Thus, it was assumed that copper-mediated induction of Fur-dependent genes was related to more indirect changes in iron-dependent cellular processes.

TABLE 6. ICP-MS measurement of total intracellular copper and iron contents under copper excess or control conditions in WT, Δ*csoR*, and Δ*copA* strains

Strain	Cu content (ppm)[a]		Cu content ratio	Fe content (ppm)		Fe content ratio
	Cu	co	(Cu/co)	Cu	co	(Cu/co)
WT	325	0.005	65,000	0.1	0.077	1.3
Δ*csoR* mutant	0.4	0.002	200	0.065	0.092	0.7
Δ*copA* mutant	892	2.0	446	0.217	0.082	2.6

[a] Cu, copper excess; co, control. Values are based on dry cell weights of samples.

Copper stress induces both iron-sulfur cluster biogenesis and cluster target genes. One major aspect of iron homeostasis is the formation of iron-sulfur cofactors. Inspection of the microarray data for regulation of iron-dependent pathways revealed that the genes involved in biogenesis of iron-sulfur cofactors were upregulated under conditions of copper excess, including the *sufU* gene, encoding the major iron-sulfur cluster scaffold protein (1), and two other putative scaffold-encoding genes, *sufA* and *sufB* (Table 7). Further, 22 of a total of 47 genes currently known to code for iron-sulfur cofactor-dependent proteins in *B. subtilis* were significantly upregulated under conditions of copper excess in both the WT and the *csoR* mutant. Two of the affected proteins, LeuC and YviD, were recently shown to be targets of copper-dependent iron-sulfur cluster distortion in *E. coli* (34). Thus, we speculated that copper stress may on one hand directly influence stability of iron-sulfur clusters bound to their target proteins but on the

TABLE 7. Effects of copper stress on iron-sulfur (Fe-S) cluster biogenesis and target gene expression in WT and Δ*csoR* mutant strains

Category and gene	Induction ratio[a]		Gene function[b]
	WT (Cu/co)	Δ*csoR*/WT (Cu)	
Fe-S biogenesis			
sufU	**2.3**	0.7	Iron-sulfur cluster scaffold
sufA	**1.9**	0.9	Iron-sulfur cluster scaffold
sufB	**1.7**	0.8	Iron-sulfur cluster maturation
sufC	**1.8**	0.8	Iron-sulfur cluster maturation
Fe-S targets			
ysfD	**2.3**	0.8	Probable glycolate oxidase subunit
lutB (*yvfW*)	**1.9**	1.0	Lactate oxidase
yhbA	**2.6**	0.8	Putative electron transport
fnr	**1.7**	1.2	Transcriptional regulator of anaerobic genes
moaA	**1.5**	0.9	Molybdopterin precursor biosynthesis
fadF	**1.6**	0.8	Putative iron-sulfur binding reductase
leuC	**2.2**	0.7	3-Isopropylmalate dehydratase (large subunit)
yrhE	**2.0**	0.5	Probable formate dehydrogenase
cysJ (*yvgQ*)	**1.7**	1.0	Sulfite reductase
yoaE	**2.7**	0.7	Probable formate dehydrogenase
skfB	**4.6**	0.8	Probable coenzyme pyrroloquinoline quinone synthesis protein
splB	**1.6**	0.8	Spore photoproduct lyase
ilvD	**2.6**	0.9	Dihydroxy-acid dehydratase
yfjO	**4.1**	0.7	Probable RNA methyltransferase
ispG (*yqfY*)	**1.6**	0.7	4-Hydroxy-3-methylbut-2-en-1-yl diphosphate synthase (involved in isoprene biosynthesis)
albA	**2.0**	0.8	Antilisterial bacteriocin (subtilosin) production
bioB	**1.9**	0.8	Biotin synthase
yotD	**11.1**	1.1	Unknown (possible rubrerythrin)
mmgE	**1.5**	1.1	Probable 2-methylcitrate dehydratase
pyrK	**2.6**	0.7	Dihydroorotate dehydrogenase (electron transfer subunit)
narG	**2.0**	0.6	Nitrate reductase (alpha subunit)
qcrA	**1.5**	0.7	Menaquinol:cytochrome *c* oxidoreductase (iron-sulfur subunit)

[a] Shown are mean induction ratios from four independent transcriptome comparisons. Cu, copper excess; co, control without added copper. Bold indicates ratios showing at least 1.5-fold upregulation, and underlining indicates ratios showing at least 1.5-fold downregulation.
[b] Gene functions are taken from the SubtiWiki database (13).

other hand also target the process of cluster assembly and transfer involving cluster scaffold proteins such as SufU. Since the SUF system is the essential iron-sulfur cluster biogenesis system in *B. subtilis*, its upregulation under copper stress gave evident support for impaired assembly already during the initial steps of cluster biogenesis. To assess whether SufU was affected on the protein level under copper stress, WT cells were grown with different concentrations of copper and a Western blot analysis was performed using total cytosolic protein fractions and SufU-specific antibodies. Indeed, a significant increase of intracellular SufU was observed in cells stressed with copper above a 0.3 mM external concentration (Fig. 2).

Copper stress leads to higher growth sensitivity and lowered Fur derepression in SufU-limited cells. In order to test the impact of copper stress on cells producing smaller amounts of SufU, a *sufU* conditional mutant was assayed for both growth and Fur-dependent gene expression. A Western blot analysis of the total cytosolic protein fraction of the conditional mutant revealed low levels of P_{xyl}-dependent *sufU* expression in the presence of 0.05% xylose and high expression in the presence of 0.5% xylose (Fig. 2). Accordingly, a xylose concentration of 0.05% was chosen for subsequent growth analysis to ensure the presence of significantly smaller SufU amounts in the mutant cells than in the WT, especially under conditions of copper excess. The WT and *sufU* conditional mutant strains, both supplied with 0.05% xylose, were grown with different copper concentrations. Final cell densities of the cultures revealed that the *sufU* conditional mutant was much more susceptible to higher concentrations of copper than the WT (Fig. 3). This indicated that the presence of larger SufU amounts was critical for proper physiological function under copper stress. To investigate if different amounts of SufU during copper stress may have an effect on cellular iron homeostasis, total RNA was isolated from *sufU* conditional mutant cultures grown with 0.5 mM copper in the presence of either 0.05% or 0.5% xylose. Dot blot analyses using mRNA antisense probes specific for

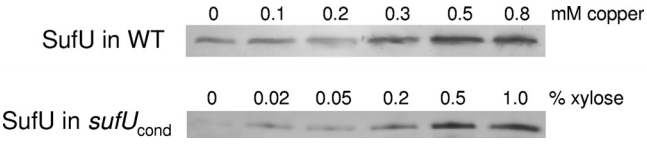

FIG. 2. Western blot detection of SufU in *B. subtilis* WT and *sufU* conditional mutant strains. *B. subtilis* WT cells were grown in minimal medium with different copper concentrations. The *sufU* conditional mutant was grown in minimal medium with different amounts of xylose, serving as inducer for *sufU* that was set under the control of the P_{xyl} promoter. Cultures were harvested at an OD_{600} of 0.8, cells were disrupted by sonication, and cytosolic protein extracts (25 μg total protein per lane) were separated by SDS-PAGE prior to blotting and detection of SufU by specific antibodies.

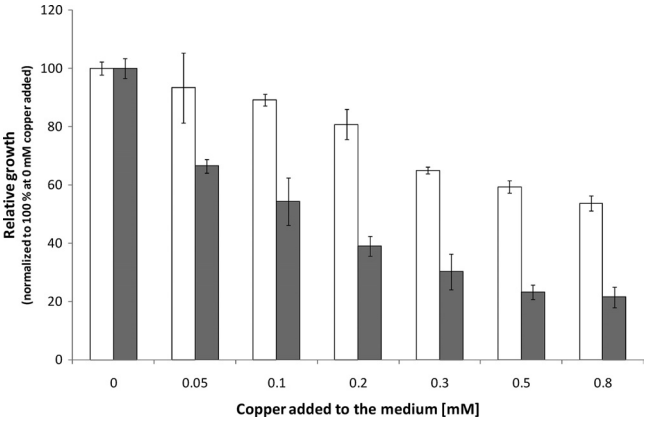

FIG. 3. Growth analysis of *B. subtilis* WT (white bars) and *sufU* conditional mutant (gray bars) strains under copper stress. Cells were grown in minimal medium with different concentrations of copper in microtiter scale with three parallels for each strain and growth condition. Final cell densities (OD_{600}) were measured after 12 h of growth. Means of the parallel determinations were normalized to the cell densities of control cultures without added copper (set to 100%) and were plotted with corresponding standard deviations.

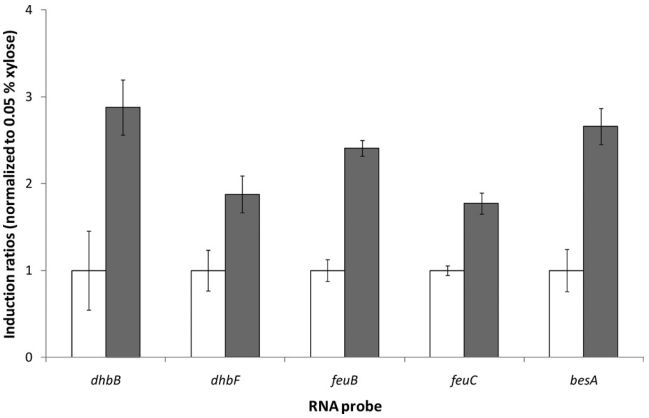

FIG. 4. Relative expression levels of Fur-regulated genes *dhbB*, *dhbF*, *feuB*, *feuC*, and *besA* in the *B. subtilis sufU* conditional mutant grown in minimal medium under conditions of copper excess (0.5 mM copper) in the presence of 0.05% xylose (white bars) or 0.5% xylose (gray bars). Total RNA was isolated from mid-log-phase cultures and analyzed by dot blot hybridization using specific mRNA antisense probes (three hybridizations each), and the signals obtained were quantified with ImageQuant software. Means of hybridization signals were normalized for each probe to those obtained from the 0.05% xylose conditions (set to 1.0) and were plotted with corresponding standard deviations.

five Fur-dependent gene transcripts were performed to detect Fur expression levels with smaller and larger amounts of intracellular SufU. The analysis revealed that mutant cells grown in the presence of 0.5% xylose showed a 2- to 3-fold-higher induction of the tested Fur-regulated genes than those grown in the presence of 0.05% xylose (Fig. 4), indicating an association of higher intracellular SufU levels and Fur derepression under the tested conditions. Thus, since SufU is an important component of intracellular iron distribution via iron-sulfur cluster assembly and targeting, it was suggested that higher requirements for iron may result not only from reduced iron-sulfur cluster stability on various target proteins but also from impaired stability during cluster assembly on SufU under copper stress.

Iron-sulfur cluster scaffolding on SufU is a direct target of copper stress *in vitro*. To assess whether copper leads to impaired cluster stability on SufU, the scaffold protein was recombinantly produced and was loaded with iron-sulfur cluster anaerobically by *in vitro* reconstitution as described previously (1). The purified holo-SufU protein carried a [4Fe-4S] cluster as the major cluster species as indicated by cluster type-specific absorption between 350 and 450 nm in the UV/visible spectrum. holo-SufU was then titrated anaerobically with increasing amounts of Cu(I) or Cu(II). With increasing amounts of Cu(I), a decrease of cluster-specific absorption was observed (Fig. 5A). Even submicromolar concentrations of Cu(I) had significant effects on cluster stability. Near the range of equimolar stoichiometries of Cu(I) (10 μM) and holo-SufU (50 μM), cluster absorbance was nearly completely abolished, indicating almost complete disintegration of the protein-bound cluster. In contrast, cluster destabilization was not observed when titrating with Cu(II) in the same molar range (Fig. 5B). This suggested that elevated levels of intracellular Cu(I) may have direct effects on iron-sulfur cluster assembly and cluster stability on SufU, which in turn had an impact on several central iron-sulfur-dependent cellular processes, as shown previously (1), and may further reflect the observed deregulation of gene expression in different pathways associated with iron and sulfur homeostasis.

DISCUSSION

While interdependent processes in homeostasis of iron and copper have been shown to occur in eukaryotes, knowledge about such processes in bacterial systems is still limited. Here, the Gram-positive model bacterium *B. subtilis* was tested for its response to copper stress. Generally, this leads to the induction of detoxification mechanisms, such as the CsoR-dependent CopZA efflux system in *B. subtilis* (53) or the CueR-regulated cytoplasmic efflux pump CopA and periplasmic copper-clearance system CueO, as well as CusRS-dependent CusCFBA, in *E. coli* (46). While copper *in vitro* leads to the initiation of Fenton-like reactions resulting in generation of ROS (20), it was thought that release of the oxidative stress defense might be another response induced by copper stress. However, the transcriptome data on copper stress in WT and copper efflux mutant strains gave another scenario of how copper stress globally affects cellular physiology. Interestingly, pathways for acquisition of iron and sulfur components were found to be upregulated, including the Fur-dependent bacillibactin pathway and cysteine biosynthesis. These findings are in agreement with a previous study on global metal ion stress (41). However, the lower Fur induction ratios observed in our study may be due to the use of *B. subtilis* ATCC 21332 (sfp^+) as the WT background, which is capable of high-affinity iron scavenging via bacillibactin. Furthermore, our study showed upregulation during copper stress of pathways that depend on the presence of iron-sulfur cofactors, such as those for branched-chain amino acid biosynthesis. The iron-sulfur cluster enzymes involved in valine, isoleucine, and leucine synthesis, IlvD and

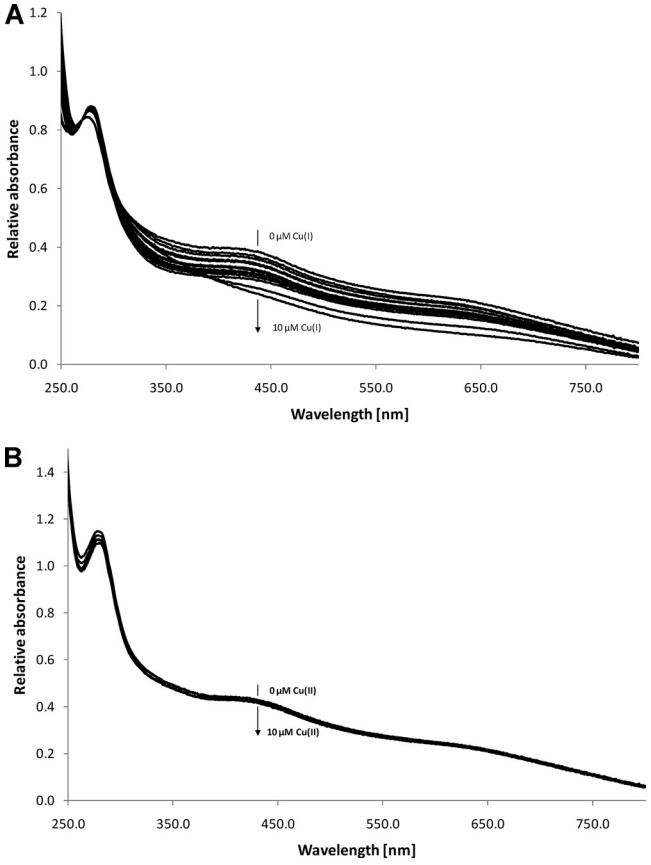

FIG. 5. Effect of copper on stability of holo-SufU *in vitro*. Recombinant SufU was reconstituted anaerobically with iron and sulfur to yield, after purification via a PD-10 size exclusion column, about 50 μM holo-SufU protein carrying a [4Fe-4S] cluster with typical absorption features ("shoulder") between 350 and 450 nm. The protein was titrated anaerobically with Cu(I) (A) or Cu(II) (B), and absorption spectra were recorded after each titration step. Cu(I) concentrations during titration were 0, 0.001, 0.006, 0.016, 0.05, 0.075, 0.1, 0.2, 0.5, 0.75, 1, 2, 5, and 10 μM, resulting in a continuous decrease of absorption of the [4Fe-4S] shoulder. Cu(II) concentrations during titration were 0, 0.01, 0.1, 1, and 10 μM, which did not result in significant bleaching of cluster absorption.

LeuC, were recently found to be targets of copper stress by systematic growth feeding experiments in *E. coli* (34). In addition to *ilvD* and *leuC*, we identified 20 other genes coding for iron-sulfur cluster-dependent proteins that were upregulated during copper excess conditions. Among them are genes encoding enzymes for biotin synthesis (BioB), molybdopterin synthesis (MoaA), pyrimidine synthesis (PyrK), and electron transfer components such as QcrA of the respiratory chain. They might not in all cases be direct targets of copper-dependent iron-sulfur cluster destabilization, as most likely in cases of IlvD and LeuC, and upregulation may involve further physiological effects associated with their metabolic function. However, since copper primarily destabilizes solvent-exposed clusters as found, e.g., in dehydratases (34), there is a further potential layer of action associated with copper toxicity. Maturation of iron-sulfur cluster proteins depends not only on cluster integrity at the final target sites but also on the upstream process of cluster biogenesis and transfer. As this study demonstrates, cluster biogenesis is also prone to destabilization by copper excess. *B. subtilis* contains the SUF system for iron-sulfur cluster assembly, with SufU as a major scaffolding protein (1). The *sufU* gene was found to be induced under conditions of copper excess together with two other potential scaffold genes, *sufA* and *sufB*, and cluster formation on recombinant SufU was revealed to be susceptible to Cu(I). Since iron-sulfur clusters are transiently bound to scaffolding proteins and are generally solvent accessible during this state of maturation (32, 42), destabilization by copper at the biogenesis level may be an effect. The data showed further that SufU *in vivo* protects cells against copper toxicity, as indicated for the SUF system in *E. coli* (34). In this context, it is interesting to note that *E. coli*, possessing both the constitutive ISC and the stress-dependent SUF cluster biogenesis systems (26), is generally less susceptible to copper stress than *B. subtilis*. Indeed, transcriptome studies in *E. coli* revealed almost no significant effects on the expression levels of Fur-regulated iron acquisition genes in the presence of 0.75 mM copper-glycine in the medium, but showed effects only in the presence of 2 mM copper-glycine, yielding expression rates similar to those observed in our study (28). Further studies showed that *E. coli* WT strains are viable at copper concentrations of above 10 mM (18, 23), whereas concentrations of above 1 to 5 mM were already lethal for *B. subtilis*. In addition to the possibility that detoxification systems are more efficient in *E. coli*, lower copper toxicity could also result from the presence of two iron-sulfur cluster biogenesis systems instead of one in *B. subtilis*, although the SUF system was shown to be more protective not only under copper stress but also under an excess of cobalt (34, 48).

Regarding the toxicity mechanism in the case of increasing intracellular copper content, copper may replace iron at the cluster binding site by occupying the cysteine-thiolate donor positions, as recently suggested (34). Indeed, it is well known that the Cu(I) and Fe(III) ion species are highly competitive (64), and the selective influence of Cu(I), which is the predominant intracellular copper species (35), may further result from its natural preference for S donor ligands, while Cu(II) prefers N donors (2). The model of metal replacement at the iron-sulfur cluster binding sites is also supported by the finding that cobalt stress also affects the function of iron-sulfur cluster proteins, including the IscU and SufA scaffolding components in *E. coli* (48). Cobalt can occupy metal binding sites with medium affinity among the physiological relevant trace metals based on the Irving-Williams series, and thus both copper and cobalt could successfully compete for thiolate donor sites if these metals are present in excess. Alternatively, it cannot be excluded that redox processes are involved in cluster destabilization, such as electron exchanges between Cu(I) and cluster-bound Fe(III). Thus, if iron-sulfur cluster assembly is not shielded from intracellular copper either by efflux systems or by cytosolic sequestration, which is mediated by metallothioneins and putatively also ferritins in several bacteria (51), cluster damage on biogenesis scaffolds can be considered a serious consequence if copper amounts exceed cellular efflux and storage capacities.

Still, the open question remains as to how copper induces the iron starvation conditions indicated by Fur derepression on global scale. Generally, several alternatives could be raised to explain the mechanism of Fur derepression. First, copper-in-

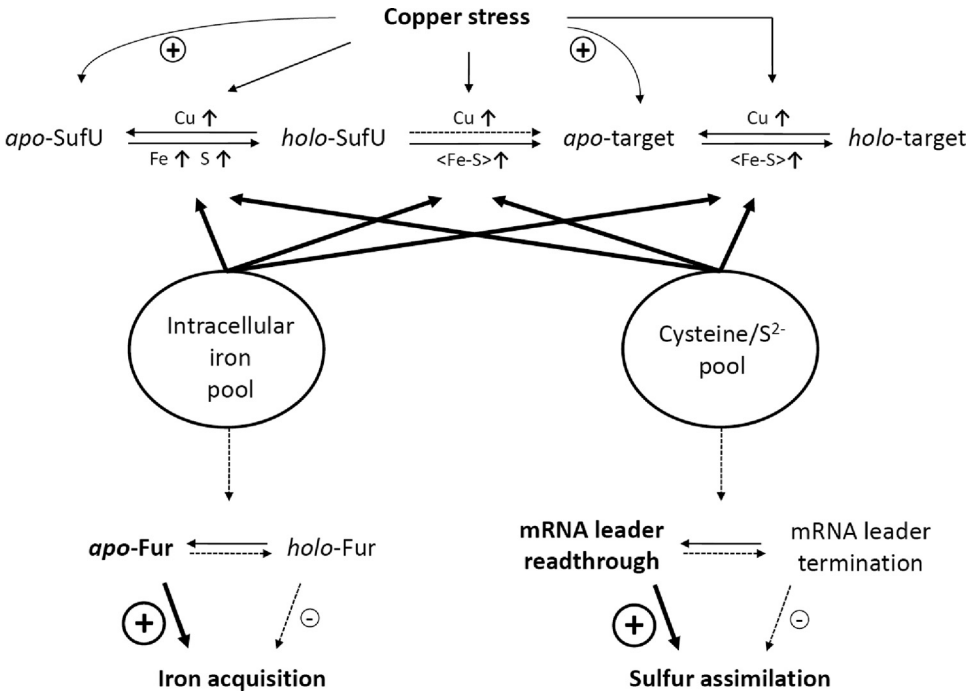

FIG. 6. Proposed model for interaction of copper, iron, and sulfur homeostasis in *B. subtilis* during copper stress. It is suggested that enhanced intracellular copper levels (Cu ↑) affect iron-sulfur cluster stability during their biogenesis involving the major scaffolding protein SufU and when they are bound on target proteins. Higher levels of biogenesis and target components generated under these conditions lead to enhanced requirements for iron (Fe ↑) and sulfur (S ↑) for stable iron-sulfur cluster formation (⟨Fe-S⟩ ↑), resulting in increased sequestration of intracellular iron and cysteine/sulfide pools within these protein components. The intracellular equilibrium displacements of the iron and cysteine/sulfide pools possibly lead to induced transcription of iron acquisition genes via Fur derepression and higher readthrough levels at S and T box mRNA leader sequences controlling the sulfur assimilation and cysteine biosynthesis pathways.

duced oxidative stress may lead to oxidation of the Fur corepressor Fe(II). However, in contrast to observations *in vitro* (20), oxidative stress was not released by copper *in vivo* and thus is unlikely to contribute to Fur derepression. This observation is in agreement with a previous study showing that copper stress does not catalyze oxidative DNA damage in *E. coli* and actually protects cells from ROS activity (35). Second, we excluded that the Fur repressor was inactivated by replacement of iron by copper, since the high intracellular copper levels found in the WT upon copper stress did not lead to full derepression of the target genes, as found for a *fur* mutant in previous studies (3), but were comparable to those found during iron limitation (<0.1 μM extracellular iron) in the bacillibactin-producing WT strain (40). Further, it was shown for *E. coli* Fur that Cu(II) binds and converts it into a repressor *in vitro* (12). Thus, if a switch from iron to copper were possible *in vivo*, a strengthened repression of the Fur regulon would be expected, which would represent the opposite effect of the observed response. The absence of this effect at all is most likely due to the intracellular Cu(I) state, which prefers a different ligand environment than Cu(II). Extracellularly induced iron limitation by decreasing iron solubility in the presence of high salinity (0.7 M NaCl) (25) can further be excluded as a relevant parameter for Fur derepression in this study, since the effective copper salt concentrations used were more than 1,000-fold lower, and intracellular total iron levels were found to be similar under both copper excess and normal conditions. Thus, since iron was sufficiently supplied to copper-stressed cultures and total intracellular iron levels were not affected, this suggests instead that an intracellular sink for iron is generated by copper stress. As copper stress was found to be associated with the upregulation of the iron-sulfur cluster assembly machinery and more than 20 iron-sulfur target genes, an iron sink could be generated by those systems, which require larger amounts of iron for proper cluster assembly under destabilizing conditions. *In vitro* studies with the SufU scaffold protein already showed that cluster formation is enhanced by increasing the iron-to-scaffold ratio severalfold (1). Data from the present study further indicate that the observed Fur derepression under copper stress is associated with increasing intracellular amounts of SufU serving as major scaffold for cluster assembly and transfer to the target proteins. In this context, the induction of sulfur assimilation and cysteine biosynthesis pathways also are thought to be linked to a higher requirement for sulfide during the cluster assembly process, which is provided by a cysteine desulfurase(s) such as SufS (Csd) as part of the SUF biogenesis machinery (1). In addition, higher cysteine contents would help to complex intracellular Cu(I), hence decreasing its toxic effect. A proposed model of interdependent copper, iron, and sulfur homeostasis based on the present data is shown in Fig. 6. It suggests a mechanism of enhanced intracellular sequestration of iron and sulfide pools by the cluster-destabilized scaffold and target components during copper stress, resulting in increased ratios of the apo-Fur repressor, which releases expression of iron acquisition genes, as well as higher portions of open S and T boxes, which control tran-

scription termination during sulfur assimilation and cysteine biosynthesis (19).

Interestingly, and as a complement to our findings, the opposite effect of increased Fur repression during copper starvation has also been observed in *Pseudomonas aeruginosa* (14). Although it is presumed that this was caused by lower demand for iron through the respiratory chain, a total knockout of all copper-dependent terminal oxidases did not change the effect of Fur target downregulation. Thus, it is possible that also under copper starvation and standard conditions, Fur regulation is influenced through different levels of intracellular copper toxicity, the onset of which was observed here at low nanomolar concentrations with holo-SufU as a target *in vitro*.

Altogether, the upregulation of physiologically important pathways during copper stress may be regarded as a recruiting strategy for components and substrates required for ensuring functional iron-sulfur cluster biogenesis also under destabilizing conditions of copper toxicity. Further investigations, especially on iron-sulfur cluster formation and transfer *in vivo*, will be necessary to obtain more insights into the processes of metal-induced iron-sulfur cluster destabilization and reconstitution.

ACKNOWLEDGMENTS

We thank Evert-Jan Blom (University of Groningen) for help with microarray studies, Erhard Bremer (University of Marburg) for help with chemifluorescence detection, Roland Lill (University of Marburg) for support with antibody production, Alexander G. Albrecht (University of Marburg) for supplying purified protein, and Jürgen Knöll and Rüdiger Penzel (University of Marburg) for help with ICP-MS measurements.

We gratefully acknowledge the Deutsche Forschungsgemeinschaft and Fonds der Chemischen Industrie for financial support.

REFERENCES

1. **Albrecht, A. G., D. J. A. Netz, M. Miethke, A. J. Pierik, O. Burghaus, F. Peuckert, R. Lill, and M. A. Marahiel.** 2010. SufU is an essential iron-sulfur cluster scaffold protein in *Bacillus subtilis*. J. Bacteriol. **192:**1643–1651.
2. **Andreini, C., L. Banci, I. Bertini, and A. Rosato.** 2008. Occurrence of copper proteins through the three domains of life: a bioinformatic approach. J. Proteome Res. **7:**209–216.
3. **Baichoo, N., T. Wang, R. Ye, and J. D. Helmann.** 2002. Global analysis of the *Bacillus subtilis* Fur regulon and the iron starvation stimulon. Mol. Microbiol. **45:**1613–1629.
4. **Baldi, P., and A. D. Long.** 2001. A Bayesian framework for the analysis of microarray expression data: regularized *t*-test and statistical inferences of gene changes. Bioinformatics **17:**509–519.
5. **Banci, L., I. Bertini, S. Ciofi-Baffoni, R. Del Conte, and L. Gonnelli.** 2003. Understanding copper trafficking in bacteria: interaction between the copper transport protein CopZ and the N-terminal domain of the copper ATPase CopA from *Bacillus subtilis*. Biochemistry **42:**1939–1949.
6. **Barbe, V., S. Cruveiller, F. Kunst, P. Lenoble, G. Meurice, A. Sekowska, D. Vallenet, T. Wang, I. Moszer, C. Medigue, and A. Danchin.** 2009. From a consortium sequence to a unified sequence: the *Bacillus subtilis* 168 reference genome a decade later. Microbiology **155:**1758–1775.
7. **Benson, A. K., and W. G. Haldenwang.** 1993. Regulation of sigma B levels and activity in *Bacillus subtilis*. J. Bacteriol. **175:**2347–2356.
8. **Bozzi, M., G. Mignogna, S. Stefanini, D. Barra, C. Longhi, P. Valenti, and E. Chiancone.** 1997. A novel non-heme iron-binding ferritin related to the DNA-binding proteins of the Dps family in *Listeria innocua*. J. Biol. Chem. **272:**3259–3265.
9. **Chen, L., and J. D. Helmann.** 1995. *Bacillus subtilis* MrgA is a Dps(PexB) homologue: evidence for metalloregulation of an oxidative-stress gene. Mol. Microbiol. **18:**295–300.
10. **Chillappagari, S., M. Miethke, H. Trip, O. P. Kuipers, and M. A. Marahiel.** 2009. Copper acquisition is mediated by YcnJ and regulated by YcnK and CsoR in *Bacillus subtilis*. J. Bacteriol. **191:**2362–2370.
11. **Cooper, D. G., C. R. Macdonald, S. J. Duff, and N. Kosaric.** 1981. Enhanced production of surfactin from *Bacillus subtilis* by continuous product removal and metal cation additions. Appl. Environ. Microbiol. **42:**408–412.
12. **de Lorenzo, V., S. Wee, M. Herrero, and J. B. Neilands.** 1987. Operator sequences of the aerobactin operon of plasmid ColV-K30 binding the ferric uptake regulation (*fur*) repressor. J. Bacteriol. **169:**2624–2630.
13. **Florez, L. A., S. F. Roppel, A. G. Schmeisky, C. R. Lammers, and J. Stülke.** 2009. A community-curated consensual annotation that is continuously updated: the *Bacillus subtilis* centred wiki SubtiWiki. Database (Oxford) **2009:** bap012.
14. **Frangipani, E., V. I. Slaveykova, C. Reimmann, and D. Haas.** 2008. Adaptation of aerobically growing *Pseudomonas aeruginosa* to copper starvation. J. Bacteriol. **190:**6706–6717.
15. **Garcia de la Nava, J., S. van Hijum, and O. Trelles.** 2003. PreP: gene expression data pre-processing. Bioinformatics **19:**2328–2329.
16. **Georgatsou, E., L. A. Mavrogiannis, G. S. Fragiadakis, and D. Alexandraki.** 1997. The yeast Fre1p/Fre2p cupric reductases facilitate copper uptake and are regulated by the copper-modulated Mac1p activator. J. Biol. Chem. **272:**13786–13792.
17. **Grass, G., and C. Rensing.** 2001. CueO is a multi-copper oxidase that confers copper tolerance in *Escherichia coli*. Biochem. Biophys. Res. Commun. **286:** 902–908.
18. **Grass, G., K. Thakali, P. E. Klebba, D. Thieme, A. Muller, G. F. Wildner, and C. Rensing.** 2004. Linkage between catecholate siderophores and the multicopper oxidase CueO in *Escherichia coli*. J. Bacteriol. **186:**5826–5833.
19. **Grundy, F. J., and T. M. Henkin.** 2002. Synthesis of serine, glycine, cysteine, and methionine, p. 245–254. *In* A. L. Sonenshein (ed.), *Bacillus subtilis* and its closest relatives. ASM Press, Washington, DC.
20. **Gunther, M. R., P. M. Hanna, R. P. Mason, and M. S. Cohen.** 1995. Hydroxyl radical formation from cuprous ion and hydrogen peroxide: a spin-trapping study. Arch. Biochem. Biophys. **316:**515–522.
21. **Harris, E. D.** 2001. Copper and iron: a landmark connection of two essential metals. J. Trace Elem. Exp. Med. **14:**207–210.
22. **Hassett, R., and D. J. Kosman.** 1995. Evidence for Cu(II) reduction as a component of copper uptake by *Saccharomyces cerevisiae*. J. Biol. Chem. **270:**128–134.
23. **Hiniker, A., J. F. Collet, and J. C. Bardwell.** 2005. Copper stress causes an *in vivo* requirement for the *Escherichia coli* disulfide isomerase DsbC. J. Biol. Chem. **280:**33785–33791.
24. **Hoch, J. A.** 1991. Genetic analysis in *Bacillus subtilis*. Methods Enzymol. **204:**305–320.
25. **Hoffmann, T., A. Schutz, M. Brosius, A. Volker, U. Volker, and E. Bremer.** 2002. High-salinity-induced iron limitation in *Bacillus subtilis*. J. Bacteriol. **184:**718–727.
26. **Johnson, D. C., D. R. Dean, A. D. Smith, and M. K. Johnson.** 2005. Structure, function, and formation of biological iron-sulfur clusters. Annu. Rev. Biochem. **74:**247–281.
27. **Kamau, P., and R. B. Jordan.** 2002. Kinetic study of the oxidation of catechol by aqueous copper(II). Inorg. Chem. **41:**3076–3083.
28. **Kershaw, C. J., N. L. Brown, C. Constantinidou, M. D. Patel, and J. L. Hobman.** 2005. The expression profile of *Escherichia coli* K-12 in response to minimal, optimal and excess copper concentrations. Microbiology **151:**1187–1198.
29. **Klein, C., C. Kaletta, N. Schnell, and K. D. Entian.** 1992. Analysis of genes involved in biosynthesis of the lantibiotic subtilin. Appl. Environ. Microbiol. **58:**132–142.
30. **Kuipers, O. P., M. M. Beerthuyzen, R. J. Siezen, and W. M. De Vos.** 1993. Characterization of the nisin gene cluster *nisABTCIPR* of *Lactococcus lactis*. Requirement of expression of the *nisA* and *nisI* genes for development of immunity. Eur. J. Biochem. **216:**281–291.
31. **Larsson, J. T., A. Rogstam, and C. von Wachenfeldt.** 2005. Coordinated patterns of cytochrome *bd* and lactate dehydrogenase expression in *Bacillus subtilis*. Microbiology **151:**3323–3335.
32. **Liu, J., N. Oganesyan, D. H. Shin, J. Jancarik, H. Yokota, R. Kim, and S. H. Kim.** 2005. Structural characterization of an iron-sulfur cluster assembly protein IscU in a zinc-bound form. Proteins **59:**875–881.
33. **London, J., and M. Knight.** 1966. Concentrations of nicotinamide nucleotide coenzymes in micro-organisms. J. Gen. Microbiol. **44:**241–254.
34. **Macomber, L., and J. A. Imlay.** 2009. The iron-sulfur clusters of dehydratases are primary intracellular targets of copper toxicity. Proc. Natl. Acad. Sci. U. S. A. **106:**8344–8349.
35. **Macomber, L., C. Rensing, and J. A. Imlay.** 2007. Intracellular copper does not catalyze the formation of oxidative DNA damage in *Escherichia coli*. J. Bacteriol. **189:**1616–1626.
36. **Mattatall, N. R., J. Jazairi, and B. C. Hill.** 2000. Characterization of YpmQ, an accessory protein required for the expression of cytochrome *c* oxidase in *Bacillus subtilis*. J. Biol. Chem. **275:**28802–28809.
37. **May, J. J., T. M. Wendrich, and M. A. Marahiel.** 2001. The *dhb* operon of *Bacillus subtilis* encodes the biosynthetic template for the catecholic siderophore 2,3-dihydroxybenzoate-glycine-threonine trimeric ester bacillibactin. J. Biol. Chem. **276:**7209–7217.
38. **Miethke, M., O. Klotz, U. Linne, J. J. May, C. L. Beckering, and M. A. Marahiel.** 2006. Ferri-bacillibactin uptake and hydrolysis in *Bacillus subtilis*. Mol. Microbiol. **61:**1413–1427.
39. **Miethke, M., S. Schmidt, and M. A. Marahiel.** 2008. The major facilitator superfamily-type transporter YmfE and the multidrug-efflux activator Mta

mediate bacillibactin secretion in *Bacillus subtilis*. J. Bacteriol. **190:**5143–5152.
40. **Miethke, M., H. Westers, E. J. Blom, O. P. Kuipers, and M. A. Marahiel.** 2006. Iron starvation triggers the stringent response and induces amino acid biosynthesis for bacillibactin production in *Bacillus subtilis*. J. Bacteriol. **188:**8655–8657.
41. **Moore, C. M., A. Gaballa, M. Hui, R. W. Ye, and J. D. Helmann.** 2005. Genetic and physiological responses of *Bacillus subtilis* to metal ion stress. Mol. Microbiol. **57:**27–40.
42. **Morimoto, K., E. Yamashita, Y. Kondou, S. J. Lee, F. Arisaka, T. Tsukihara, and M. Nakai.** 2006. The asymmetric IscA homodimer with an exposed [2Fe-2S] cluster suggests the structural basis of the Fe-S cluster biosynthetic scaffold. J. Mol. Biol. **360:**117–132.
43. **Mostertz, J., C. Scharf, M. Hecker, and G. Homuth.** 2004. Transcriptome and proteome analysis of *Bacillus subtilis* gene expression in response to superoxide and peroxide stress. Microbiology **150:**497–512.
44. **Ollinger, J., K. B. Song, H. Antelmann, M. Hecker, and J. D. Helmann.** 2006. Role of the Fur regulon in iron transport in *Bacillus subtilis*. J. Bacteriol. **188:**3664–3673.
45. **Osaki, S., and D. A. Johnson.** 1969. Mobilization of liver iron by ferroxidase (ceruloplasmin). J. Biol. Chem. **244:**5757–5758.
46. **Outten, F. W., D. L. Huffman, J. A. Hale, and T. V. O'Halloran.** 2001. The independent *cue* and *cus* systems confer copper tolerance during aerobic and anaerobic growth in *Escherichia coli*. J. Biol. Chem. **276:**30670–30677.
47. **Peuckert, F., M. Miethke, A. G. Albrecht, L. O. Essen, and M. A. Marahiel.** 2009. Structural basis and stereochemistry of triscatecholate siderophore binding by FeuA. Angew. Chem. Int. Ed. Engl. **48:**7924–7927.
48. **Ranquet, C., S. Ollagnier-de-Choudens, L. Loiseau, F. Barras, and M. Fontecave.** 2007. Cobalt stress in *Escherichia coli*. The effect on the iron-sulfur proteins. J. Biol. Chem. **282:**30442–30451.
49. **Raymond, K. N., E. A. Dertz, and S. S. Kim.** 2003. Enterobactin: an archetype for microbial iron transport. Proc. Natl. Acad. Sci. U. S. A. **100:**3584–3588.
50. **Reents, H., R. Munch, T. Dammeyer, D. Jahn, and E. Hartig.** 2006. The Fnr regulon of *Bacillus subtilis*. J. Bacteriol. **188:**1103–1112.
51. **Robinson, N. J.** 2008. A bacterial copper metallothionein. Nat. Chem. Biol. **4:**582–583.
52. **Sambrook, J., E. F. Fritsch, and T. Maniatis.** 1989. Molecular cloning: a laboratory manual, 2nd ed. Cold Spring Harbor Laboratory Press, Cold Spring Harbor, NY.
53. **Smaldone, G. T., and J. D. Helmann.** 2007. CsoR regulates the copper efflux operon *copZA* in *Bacillus subtilis*. Microbiology **153:**4123–4128.
54. **Spizzo, T., C. Byersdorfer, S. Duesterhoeft, and D. Eide.** 1997. The yeast FET5 gene encodes a FET3-related multicopper oxidase implicated in iron transport. Mol. Gen. Genet. **256:**547–556.
55. **Stearman, R., D. S. Yuan, Y. Yamaguchi-Iwai, R. D. Klausner, and A. Dancis.** 1996. A permease-oxidase complex involved in high-affinity iron uptake in yeast. Science **271:**1552–1557.
56. **Stoj, C., and D. J. Kosman.** 2003. Cuprous oxidase activity of yeast Fet3p and human ceruloplasmin: implication for function. FEBS Lett. **554:**422–426.
57. **Stülke, J., R. Hanschke, and M. Hecker.** 1993. Temporal activation of beta-glucanase synthesis in *Bacillus subtilis* is mediated by the GTP pool. J. Gen. Microbiol. **139:**2041–2045.
58. **Thieme, D., and G. Grass.** 2010. The Dps protein of *Escherichia coli* is involved in copper homeostasis. Microbiol. Res. **165:**108–115.
59. **Vagner, V., E. Dervyn, and S. D. Ehrlich.** 1998. A vector for systematic gene inactivation in *Bacillus subtilis*. Microbiology **144:**3097–3104.
60. **van Bakel, H., E. Strengman, C. Wijmenga, and F. C. Holstege.** 2005. Gene expression profiling and phenotype analyses of *S. cerevisiae* in response to changing copper reveals six genes with new roles in copper and iron metabolism. Physiol. Genomics **22:**356–367.
61. **van Hijum, S. A., J. Garcia de la Nava, O. Trelles, J. Kok, and O. P. Kuipers.** 2003. MicroPreP: a cDNA microarray data pre-processing framework. Appl. Bioinformatics **2:**241–244.
62. **Vulpe, C. D., Y. M. Kuo, T. L. Murphy, L. Cowley, C. Askwith, N. Libina, J. Gitschier, and G. J. Anderson.** 1999. Hephaestin, a ceruloplasmin homologue implicated in intestinal iron transport, is defective in the *sla* mouse. Nat. Genet. **21:**195–199.
63. **Wach, A.** 1996. PCR-synthesis of marker cassettes with long flanking homology regions for gene disruptions in S. cerevisiae. Yeast **12:**259–265.
64. **Waldron, K. J., and N. J. Robinson.** 2009. How do bacterial cells ensure that metalloproteins get the correct metal? Nat. Rev. Microbiol. **7:**25–35.